(3) J. D. Ferry, E. L. Foster, G. V. Browning, and W. M. Sawyer, *J. Colloid Sci.*, **6**, 377 (1951).
(4) M. F. Johnson, W. W. Evans, I. Jordan, and J. D. Ferry, *J. Colloid Sci.*, **7**, 498 (1952).
(5) J. D. Ferry, L. D. Grandine, Jr., and D. C. Udy, *J. Colloid Sci.*, **8**, 529 (1953).
(6) S. Onogi, S. Kimura, T. Kato, T. Masuda, and N. Miyanaga, *J. Polym. Sci., Part C*, **15**, 381 (1966).
(7) K. S. Gandhi and M. C. Williams, *J. Polym. Sci., Part C*, **35**, 211 (1971).
(8) K. S. Gandhi and M. C. Williams, *J. Appl. Polym. Sci.*, **16**, 2721 (1972).
(9) O. Quadrat and J. Podnecká, *Collect. Czech. Chem. Commun.*, **37**, 2402 (1972).
(10) V. E. Dreval, A. Ya. Malkin, and G. V. Vinogradov, *Eur. Polym. J.*, **9**, 85 (1973).
(11) (a) H. Kajiura, Y. Ushiyama, T. Fujimoto, and M. Nagasawa, *Macromolecules*, **11**, 894 (1978); (b) G. C. Berry, H. Nakayasu, and T. G. Fox, *J. Polym. Sci., Polym. Phys. Ed.*, **17**, 1825 (1979).
(12) Y. Isono, T. Fujimoto, H. Kajiura, and M. Nagasawa, *Polym. J.*, **12**, 363 (1980).
(13) J. P. Cotton, D. Decker, H. Benoit, B. Farnoux, J. Higgins, G. Jannink, R. Ober, C. Picot, and J. des Cloizeaux, *Macromolecules*, **7**, 863 (1974).
(14) M. Daoud, J. P. Cotton, B. Farnoux, G. Jannink, G. Sarma, H. Benoit, R. Duplessix, C. Picot, and P. G. de Gennes, *Macromolecules*, **8**, 804 (1975).
(15) H. Hayashi, F. Hamada, and A. Nakajima, *Makromol. Chem.*, **178**, 827 (1977).
(16) H. Hayashi, F. Hamada, and A. Nakajima, *Polymer*, **18**, 638 (1977).
(17) H. Kajiura, M. Sakai, and M. Nagasawa, *Trans. Soc. Rheol.*, **20**, 575 (1976).
(18) T. Fujimoto, N. Ozaki, and M. Nagasawa, *J. Polym. Sci., Part A-2*, **6**, 129 (1968).
(19) M. Sakai, T. Fujimoto, and M. Nagasawa, *Macromolecules*, **5**, 786 (1972).
(20) T. Kato, K. Miyaso, I. Noda, T. Fujimoto, and M. Nagasawa, *Macromolecules*, **3**, 777 (1970).
(21) A. R. Schultz and P. J. Flory, *J. Am. Chem. Soc.*, **74**, 4760 (1952).
(22) S. H. Maron, I. M. Krieger, and A. W. Sisko, *J. Appl. Phys.*, **25**, 971 (1954).
(23) H. Endo and M. Nagasawa, *J. Polym. Sci., Part A-2*, **8**, 371 (1970).
(24) H. Kajiura, H. Endo, and M. Nagasawa, *J. Polym. Sci., Polym. Phys. Ed.*, **11**, 2371 (1973).
(25) G. C. Berry, *J. Chem. Phys.*, **46**, 1338 (1967).
(26) G. C. Berry, B. L. Hager, and C. P. Wong, *Macromolecules*, **10**, 361 (1977).
(27) W. W. Graessley, *J. Chem. Phys.*, **43**, 2696 (1965); **47**, 1942 (1967).
(28) Y. Isono, H. Kajiura, and M. Nagasawa, *J. Rheol.*, **23**, 79 (1979).

# Rheooptical Studies of Racemic Poly($\gamma$-benzyl glutamate) Liquid Crystals

**Tadahiro Asada,* Hiromochi Muramatsu, Ryoji Watanabe, and Shigeharu Onogi**

*Department of Polymer Chemistry, Kyoto University, Kyoto 606, Japan.*
*Received June 21, 1979*

ABSTRACT: Both the rheooptical and rheological properties of a polymer liquid crystalline system may well be interpreted by supposing three typical structural models for the bulk structure of the system: (1) a piled polydomain, in which many small domains are piled randomly; (2) a dispersed polydomain, in which a large domain occupies the whole volume, but not without the presence of some smaller domains; (3) a monodomain continuous phase. The piled polydomain which is usually seen for a virgin sample is considered to be transformed finally into a monodomain continuous phase by a shear or other external field. The flow properties of concentrated solutions of racemic poly($\gamma$-benzyl glutamate) in *m*-cresol at concentrations above the *B* point have been observed with a rheometer equipped with a quartz cone-plate and the transmitted light intensities ($I_x$, $I_\parallel$, $I_E$) of polarized light have been simultaneously measured as a function of shear rate.

Studies[1-8] of the rheological behavior of polymer liquid crystals provide a great deal of technologically important information, particularly information about the ability to spin such materials into fibers, but rheological methods alone cannot give the full picture. Such materials form complicated and unstable superstructures and accompanying unusual textures. Therefore, new rheooptical techniques were developed in our laboratory for studying the relation between structure and rheological properties of various liquid crystals.[9-12] This paper is concerned with the rheooptical properties of solutions of poly($\gamma$-benzyl glutamate) in the liquid-crystal state.

## Experimental Section

**Measurements.** A block diagram of one of the rheooptical instruments (apparatus II) is shown in Figure 1. A cone and plate type rheometer equipped with a transparent cone and plate made of quartz is combined with the optical system. A monochromatic laser light beam ($\lambda$ = 6328 Å) passes through a polarizer (P), quartz plate (E), sample (F), quartz cone (G), and analyzer (A). The transmitted light is finally detected by a photomultiplier tube ($PM_l$). Thus, the apparatus enables us to simultaneously measure rheological properties and transmission of polarized lights through a sheared sample. The diameters of the cones and plates employed were kept constant (8 cm). Four cones of different cone angles (0.865, 1.01, 2.06, 3.85°) were used.

At room temperature (22 °C), the shear stress and transmitted light intensities ($I_x$, $I_\parallel$, $I_E$) were measured simultaneously as functions of shear rate ($3 \times 10^{-2}$–$2 \times 10^2$ $s^{-1}$), where $I_x$, $I_\parallel$, and $I_E$ are fractional transmitted light intensities when crossed polarizers (at $\psi$ = 45° in Figure 2), parallel polarizers (at $\psi$ = 45°), and crossed polarizers at the extinction position (at $\psi$ = 0°) are used, respectively. The geometries are shown in Figure 2.

Although it depended on concentration and shear rate whether or not the optical quantities varied with time at constant shear rate, all data presented here were taken at the steady state, and these were confirmed by observing for a much longer time than that required for recognizing the steady state of the stress: for example, 60 min at $\dot{\gamma} = 3.47 \times 10^{-2}$ $s^{-1}$, 30 min at $\dot{\gamma} = 6.9 \times 10^{-1}$ $s^{-1}$, and 1 min at $\dot{\gamma} = 1.04 \times 10^2$ $s^{-1}$.

**Materials.** Poly($\gamma$-benzyl L-glutamate) of weight-average molecular weight $15 \times 10^4$ and poly($\gamma$-benzyl D-glutamate) of weight-average molecular weight $15 \times 10^4$ were obtained from Sigma Chemical Co. These weight-average molecular weights $\bar{M}_w$ were estimated from the intrinsic viscosity [$\eta$] of dilute solutions in dichloroacetic acid at 25 °C, using the relation proposed by Doty et al.[13] Equal amounts of both materials were dissolved in

0024-9297/80/2213-0867$01.00/0 

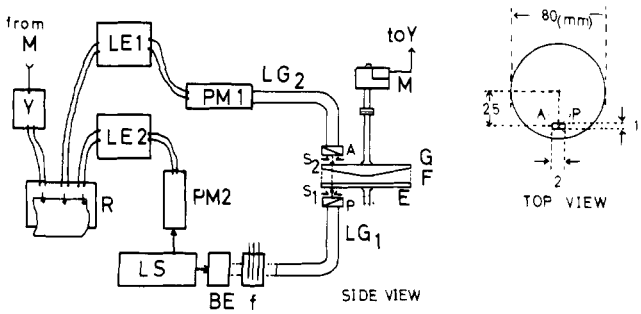


**Figure 1.** Block diagram of rheooptical apparatus II: LS, laser light source; BE, beam expander; F, filter, $LG_1$, input glass fiber tube (light guide, 10-mm i.d. × 30 μm); P, polarizer; $S_1$, entrance slit; E, quartz plate; F, sample, G, quartz cone; $S_2$, exit slit; A, analyzer; $LG_2$, output glass fiber tube; $PM_1$, photomultiplier tube; $LE_1$, amplifier; $PM_2$, photomultiplier tube (for monitor use); $LE_2$, amplifier (for monitor use); R, recorder; M, transducer for detecting torque; Y, amplifier (for torque).

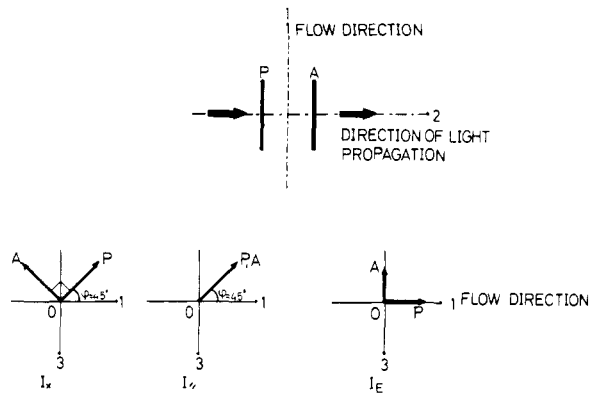


**Figure 2.** Geometry of the optical system: 1, flow direction; 2, direction of light propagation; 3, radial direction of the cone and plate. $\overrightarrow{OP}$ is the transmission axis of the polarizer and $\overrightarrow{OA}$ is the transmission axis of the analyzer.

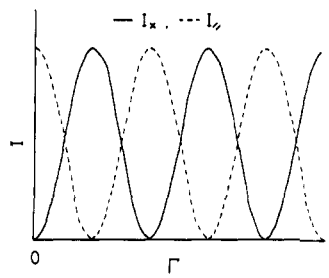


**Figure 3.** Schematic representation of the variation of transmitted light intensities ($I_x$, $I_\parallel$) with retardation (Γ) according to eq 1.

*m*-cresol to give 20, 30, and 40 wt % solutions. The concentrations of these solutions are above the *B* point at 22 °C.

**General Considerations of the Optical Quantities. (1) Uniform System.** When the retardation (Γ) of a uniaxially oriented continuous phase undergoes continuous changes, $I_x$ and $I_\parallel$ vary in a quasi-periodic manner, as expressed by eq 1 and shown

$$I_x = K \sin^2 (\pi\Gamma/\lambda)$$

$$I_\parallel = K[1 - \sin^2 (\pi\Gamma/\lambda)] \quad (1)$$

schematically in Figure 3. In eq 1 λ is the wavelength of the light and *K* is a coefficient which is unity when there is no absorption and scattering. In such a simple case, this equation enables us to evaluate birefringence from $I_x$ and $I_\parallel$ (the so-called transmission method[14]). The same idea can be applied to a liquid-crystal system, as long as the system is optically inactive and behaves as a monodomain continuous phase [schematically shown in Figure 6 (III)].

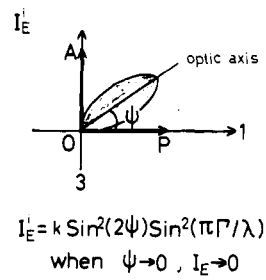


$$I_E^i = k \sin^2(2\psi)\sin^2(\pi\Gamma/\lambda)$$

when $\psi \to 0$, $I_E \to 0$

**Figure 4.** A uniaxially birefringent subdomain between crossed polarizers. Transmission axis of the polarizer ($\overrightarrow{OP}$) coincides with flow direction 1. ψ is the angle between the optical axis and the polarizer axis. The transmitted light intensity $I_E^i$ should be 0 when $\psi \to 0$.

If there is an optical rotational effect due to molecular or structural optical activity, this effect may be superimposed on the birefringent effect. In such a case $I_E$ is helpful to know whether or not the optical rotational effect is involved, because a change in optical rotational power causes a wavy change of $I_E$. On the other hand, for a uniaxially birefiringent system without optical rotation, $I_E$ should be zero. When the optical rotational effect is very small, the birefringence can still be evaluated by the transmission method.[14] Actually, we have obtained the streaming birefringence of isotropic solutions of poly(γ-benzyl L-glutamate) successfully by this transmission method.[11]

**(2) Polydomain System of Liquid Crystals.** Generally, liquid crystals appear in so-called polydomain textures (for example, Figure 4 in ref 10). Lyotropic polymer liquid crystals also appear in polydomain textures (for example, Figure 4 in ref 15). For such polydomain textures, many domains exist in a field. The incident polarized light will be depolarized by various degrees owing to the depolarization effect of various domains.[12] No difference between $I_x$ and $I_\parallel$ will be observed, since the transmitted light consists of variously depolarized lights. Thus for such polydomain systems, it is difficult to obtain birefringence as a measure of molecular orientation by the transmission method.

As mentioned above, $I_E$ is useful for studying the deformation process in such polydomain systems. Suppose a uniaxially birefringent body is put between crossed polarizers as shown in Figure 4. The transmission axis of the polarizer ($\overrightarrow{OP}$) coincides with the flow direction 1. The angle between the optical axis and the polarizer axis (transmission axis of the polarizer) is denoted by ψ. When the uniaxially birefringent body orients such that its optical axis is parallel to the flow direction, the angle ψ becomes zero, and hence the transmitted light intensity $I_E$ tends to zero. Thus, for an ideal system without light scattering and optical activity, $I_E = 0$ means that all subdomains orient so that their optical axes are parallel to the flow direction or that all subdomains coalesce to a monodomain continuous phase having the optic axis parallel to the flow direction. Here, a volume element which acts as a birefringent body is referred to as a subdomain.

Now, consider a case in which several domains exist in a field. The thickness and the direction of the optical axes of the subdomains are randomly distributed. Consequently, the incident light will be depolarized during the passage. Thus, a high value, say 50%, will be expected for all three optical quantities $I_E$, $I_x$, and $I_\parallel$.

## Results and Discussion

The optical quantities hereafter will be represented by the percent transmission with respect to the light intensity transmitted through parallel polarizers for isotropic solutions. It was found that the optical quantities at the steady state as function of shear rate depend on the sample thickness. In order to clarify this effect quantitatively, we measured $I_x$ and $I_\parallel$ by using a parallel-plate rheometer rather than a cone–plate one. The results are shown in Figure 5. In this figure, *d* denotes the sample thickness. As is evident from the figure, $I_x$ and $I_\parallel$ show periodic change with large amplitudes at higher shear rates. The thinner the sample and the higher the shear rate, the more

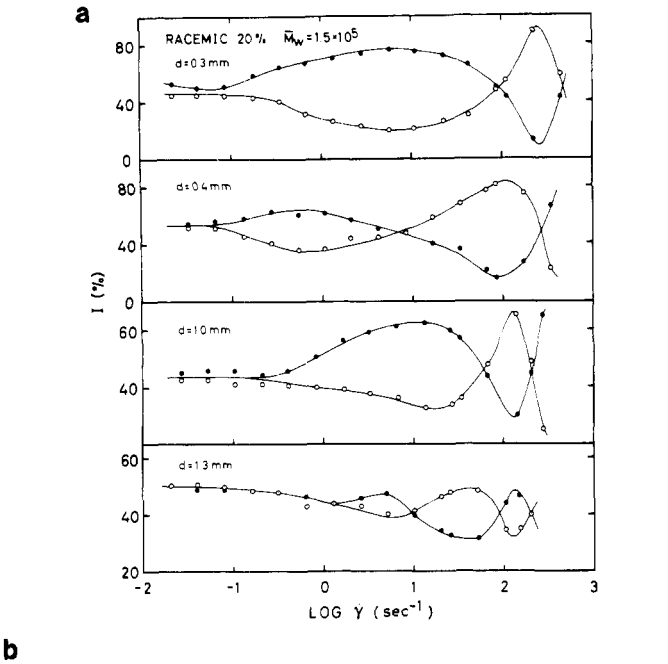


**Figure 5.** Thickness effect of rheooptical property for 20% solution. (a) $I_x$ (○) and $I_\parallel$ (●), the transmitted light intensities illustrated in Figure 2, are plotted against the log of the shear rate ($\dot{\gamma}$). $d$ is the thickness of the sample between the plates. (b) $I_E$, the transmitted light intensity illustrated in Figure 2, is plotted against the log of the shear rate ($\dot{\gamma}$): (○) $d$ = 0.3 mm; (Φ) $d$ = 0.4 mm; (⊖) $d$ = 0.6 mm; (●) $d$ = 1.0 mm.

striking is the waviness. On the other hand, $I_E$ is very low at higher shear rates. On the contrary, at lower shear rates, $I_x$ and $I_\parallel$ are almost constant and $I_E$ is very high.

As discussed previously (General Considerations of Optical Quantities), the periodic changes in $I_x$ and $I_\parallel$ mean that the continuous change in retardation with shear rate takes place and that there exists a continuous phase which contributes to the retardation change. If there are domains suspended in the continuous phase, the wavy change in $I_x$ and $I_\parallel$ will be masked by their depolarization effects; correspondingly $I_E$ will become larger. So long as the masking effect is not too great, the amplitude of the wavy curve will be reduced slightly. On the contrary, when the masking effect is extremely large, the wavy change in $I_x$ and $I_\parallel$ might not be observed.

The results seen in Figure 5 are well interpreted by the structural models shown schematically in Figure 6. The values of $I_x$, $I_\parallel$ and $I_E$ for a virgin state of the sample are always approximately 50%, though they are not shown in the figures. This fact means that the incident light was depolarized almost completely and the transmitted light contains various components of electric vectors. Such a polydomain system which consists entirely of small do-

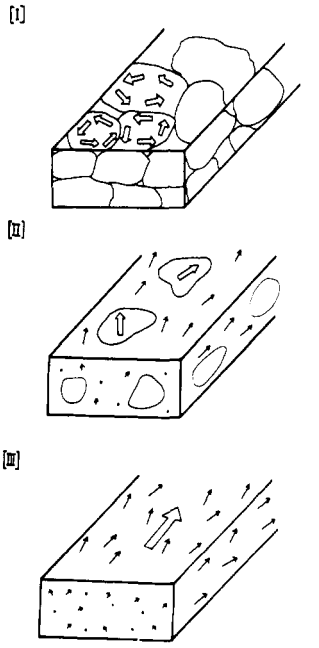


**Figure 6.** Schematic representations of liquid crystalline structures of a polymeric system: (I) piled polydomain system; (II) dispersed polydomain system; (III) monodomain continuous phase.

mains is referred to here as a "piled polydomain system" [shown schematically in Figure 6 (I)]. For an undeformed piled polydomain system, $I_E$ will be very large. The wavy change in $I_x$ and $I_\parallel$ would not be expected if the piled polydomain structure were maintained during the flow. The flow maintaining the piled polydomain structure was referred to before as "polydomain flow"; this was observed under the microscope with concentrated poly(γ-benzyl L-glutamate) solutions by us[12] and with [poly(1,4-phenyleneterephthalamide) and poly[(2,7-phenanthridone) terephthalamide] solutions by Horio.[15]

At higher shear rate for thinner samples, the system is considered to flow almost as a monodomain continuous phase [Figure 6 (III)], because $I_x$ and $I_\parallel$ show periodic changes with large amplitudes and at the same time $I_E$ is very small. The initial polydomain structure is transformed to a monodomain continuous phase by shear deformation with a high shear rate. Here we must take into account the coalescence and growing of individual domains by shear.

A domain will be deformed by applied shear and grow larger by coalescence with neighboring domains. As a consequence of the successive occurrence of such a coalescence and growing process, a continuous phase appears which initially contains a number of remaining domains. The remaining domains will coalesce into the continuous phase after all, provided the shear rate becomes large enough. Thus it can be said that the initial piled polydomain structure is transformed to a dispersed polydomain system above a certain shear rate (or stress). When the continuous phase predominates in the sample, the wavy change in $I_x$ and $I_\parallel$ can be observed.

At lower shear rates where both $I_x$ and $I_\parallel$ are almost constant and $I_E$ is very high, the system is considered to flow, maintaining its piled polydomain structure or a dispersed polydomain system just transformed from a piled polydomain structure. Above a critical shear rate ($\dot{\gamma}_i$), at which the wavy change of $I_x$ and $I_\parallel$ starts, the continuous phase appears predominantly in the sample. The increasing amplitude of the wavy curve with increasing shear

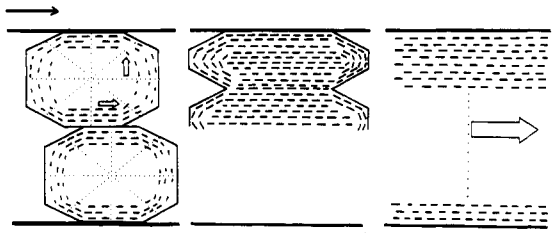

**Figure 7.** Schematic illustration of domain-uniting. Solid rod represents the director.

rate implies that the volume fraction of the continuous phase in the dispersed polydomain system [Figure 6 (II)] increases with increasing shear rate.

The decrease of $I_E$ in Figure 5b corresponds to the increase of the amplitude of wavy curve in Figure 5a; $I_E$ varies with shear rate as if it envelopes wavy curves of $I_x$ and $I_\parallel$. The variation of $I_E$ with shear rate also represents the variation of the fraction of suspended domains in the sample by coalescence and growing. Figure 5b shows that above the critical shear rate ($\dot{\gamma}_i$) $I_E$ decreases with increasing shear rate; above a higher critical shear rate ($\dot{\gamma}_e$) it approaches a low equilibrium value which depends on the thickness. The thicker the sample, the higher the critical shear rate. It is reasonable to attribute this equilibrium of $I_E$ at high shear rates to a monodomain-oriented continuous phase formed throughout the sample. The monodomain continuous phase may still contain some defects, which cause the depolarizing effect, and, hence, a nonzero equilibrium value of $I_E$.

If the deformation of all domains in the sample were uniform, $\dot{\gamma}_e$ should be independent of sample thickness. However, this is not the case when one observes the experimental results. Therefore, we must consider the wall effect[16-20] or inequality of deformation of domains. In the case of thinner samples, the majority of domains contact the walls directly and are sheared effectively. For thicker samples, on the other hand, domains in direct contact with the walls are sheared effectively, but may other domains are not so sheared because rotation or slippage of domains occurs. These domains can coalesce into a continuous phase only at much higher shear rates.

The coalescence or growing process of domains is schematically illustrated in Figure 7. In the unsheared state (left), the system consists of many domains oriented randomly. The territories which are surrounded by the solid lines are what we call "domain" and the domain consists of several subdomains. A subdomain can be treated as a single birefringent volume element which is observed as a dark or bright region under a crossed-polarizer microscope. In this figure, the solid rods in a domain represent directors which indicate the local orientation of molecules. The white arrows in the figure show the average orientation directions of the directors. When the domains are deformed by an applied force, as in the center of Figure 7, there appear regions where directors of adjacent domains coincide with each other. Then these adjacent domains coalesce into a large domain. Thus, the domains become larger and larger until they grow to a monodomain continuous phase (right). In an intermediate stage, some domains or domainlets remain in a continuous phase [Figure 6 (II)].

For 20% solution, wavy changes of $I_x$ and $I_\parallel$ and the decrease in $I_E$ begin at a very low shear rate ($\dot{\gamma}_i = 8 \times 10^{-2}$ $s^{-1}$). At high shear rates, the amplitude of the wavy curves becomes very large, and $I_E$ approaches asymptotically a very low value. From these results for the 20% solution, we conclude that the piled polydomain structure in the undisturbed state changes easily to a continuous phase,

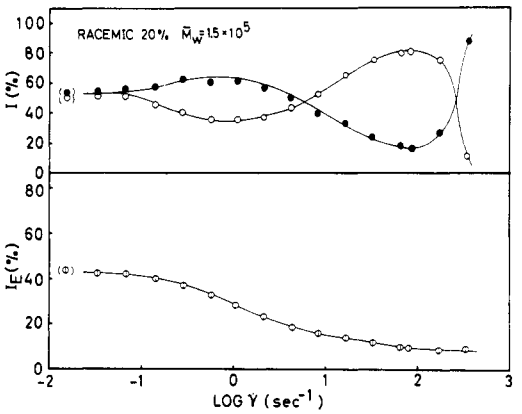


**Figure 8.** Variations of $I_x$ (○), $I_\parallel$ (●), and $I_E$ (⊙) with shear rate ($\dot{\gamma}$) for a 20% solution.

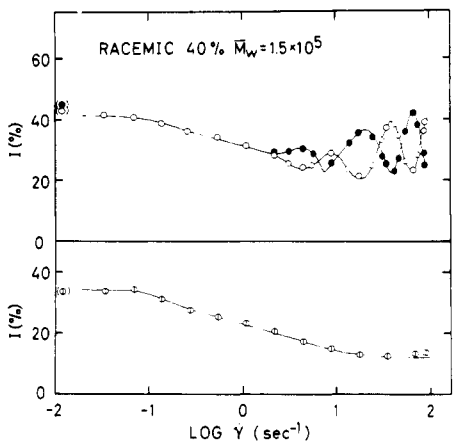


**Figure 9.** Variations of $I_x$ (○), $I_\parallel$ (●), and $I_E$ (⊙) with shear rate ($\dot{\gamma}$) for a 40% solution.

even at low shear rates, and the continuous phase grows with increasing shear rate until it forms a monodomain continuous phase at high shear rate ($1 \times 10^2$ $s^{-1}$).

The rheooptical behavior of a 30% solution is almost the same as that of a 20% solution, except that the critical shear rate $\dot{\gamma}_i$ is 1 $s^{-1}$, higher than that for 20% solution.

For a 40% solution, $I_E$ begins to decrease at a lower shear rate ($\dot{\gamma}_i = 7 \times 10^{-2}$ $s^{-1}$), above which both $I_x$ and $I_\parallel$ decrease with increasing shear rate, in marked contrast to the case for a 20% solution. The decrease in $I_E$ here does not indicate the disappearance or orientation of the polydomain structure but does mean that dynamic light scattering due to polydomain flow will occur. Such rheooptical behavior of a 40% solution is similar to that of thicker sample of a 20% solution, except for the remarkable decrease in $I_x$ and $I_\parallel$ with increasing shear rate. This result may be interpreted by considering that the domains in a 40% solution are smaller than those in less concentrated solutions and hence more domains are included in the same thickness.

In Figure 10, flow properties of the three solutions are shown. It should be emphasized here that no differences were observed in the flow properties measured at different cone angles, although the rheooptical properties measured simultaneously depend strongly on the cone angle, as mentioned previously. The apparent viscosity ($\eta$) curve for a 30% solution is similar to that for a 20% solution. The apparent viscosities of these solutions do not depend on shear rates below $\dot{\gamma} = 1 \times 10^2$ $s^{-1}$, while that of a 40% solution depends strongly on shear rate in the entire region examined.

Presumably, at very low shear rates, shear-rate dependence of the apparent viscosity for the 20 and 30% solu-

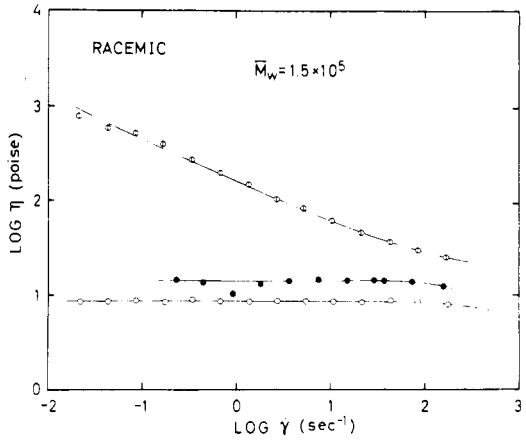


**Figure 10.** Apparent viscosities as a function of shear rate ($\dot{\gamma}$): (○) 20%; (●) 30%; (⊙) 40%.

tions would be observed. The decrease in the apparent viscosity for a 40% solution with increasing shear rate may arise from plastic flow of piled domains, each of which has a very high yield value. On the contrary, the yielding of domain in 20 and 30% solutions may occur at so small a stress that it cannot be detected. From the above results system a 40% solution, we conclude that domains in concentrated solutions are smaller and more stable than those in less concentrated solutions. The higher mechanical stability of the domains in a 40% solution is also considered to be responsible for the decrease of transmission of light with increasing shear rate due to dynamic scattering, as mentioned earlier.

We point out that no long-range orientation would be expected, so long as polydomain flow takes place. To attain uniform molecular orientation throughout a sample, one must find conditions where a continuous monodomain phase truly exists. Piled polydomain will be transformed to a monodomain continuous phase by shear or other external field. To obtain a highly oriented system (i.e., to obtain an oriented monodomain continuous phase), one must induce the domains to coalesce and grow larger. For this purpose, the applied stress (or strain) must be delivered effectively to individual domains. Consequently, to get a highly oriented sample, it is necessary to take into account the mode of deformation, including the geometry of the apparatus as well as the size and stability of domains, which probably depend on molecular weight, concentration, temperature, pressure, and so on.

The above results show that domains for higher concentration are small and mechanically stable and that a higher shear rate (or larger stress) is required to obtain an oriented monodomain continuous phase. On the other hand, for lower concentrations only a low shear rate (or small stress) is required because domains are large and unstable, provided all other conditions such as geometrical conditions of the apparatus, temperature, and so on are the same.

## References and Notes

(1) J. T. Yang, *J. Am. Chem. Soc.*, **80**, 1783 (1958).
(2) J. Hermans, *J. Colloid Sci.*, **17**, 638 (1962).
(3) S. P. Papkov, V. G. Kulichikhin, V. D. Kalmykova, and A. Y. Malkin, *J. Polym. Sci., Polym. Phys. Ed.*, **12**, 1753 (1974).
(4) W. J. Jackson and H. F. Kuhfuss, *J. Polym. Sci., Polym. Chem. Ed.*, **14**, 2043 (1976).
(5) J. L. White and J. F. Fellers, *J. Appl. Polym. Sci., Appl. Polym. Symp.*, **No. 33**, 137 (1978).
(6) H. Aoki, D. R. Coffin, T. A. Hancock, D. Harwood, R. S. Lenk, J. F. Fellers, and J. L. White, *J. Polym. Sci., Polym. Symp.*, **No. 65**, 29 (1978).
(7) C. P. Wong, H. Ohnuma, and G. C. Berry, *J. Polym. Sci., Polym. Symp.*, **No. 65**, 175 (1978).
(8) G. Kiss and R. S. Proter, *J. Polym. Sci., Polym. Symp.*, **No. 65**, 193 (1978).
(9) T. Asada, Y. Maruhashi, and S. Onogi, *Nippon Reoroji Gakkaishi*, **3**, 129 (1975).
(10) T. Asada, *Nippon Reoroji Gakkaishi*, **4**, 102 (1976).
(11) T. Asada, Y. Maruhashi, Y. Kuroki, and S. Onogi, *Nippon Reoroji Gakkaishi*, **6**, 14 (1978).
(12) T. Asada, H. Muramatsu, and S. Onogi, *Nippon Reoroji Gakkaishi*, **6**, 130 (1978).
(13) P. Doty, J. H. Bradbury, and A. M. Hultzer, *J. Am. Chem. Soc.*, **78**, 947 (1956).
(14) R. S. Stein, S. Onogi, K. Sasaguri, and D. A. Keedy, *J. Appl. Phys.*, **34**, 80 (1963).
(15) M. Horio, *Koenshu—Kyoto Daigaku Nippon Kagaku Sen'i Kenkyusho*, **35**, 87 (1978).
(16) S. Peter and H. Peters, *Z. Phys. Chem. (Wiesbaden)*, **3**, 103 (1955).
(17) R. S. Porter, E. M. Barrall II, and J. F. Johnson, *J. Chem. Phys.*, **45**, 1452 (1966).
(18) R. S. Porter and J. F. Johnson, "Rheology", F. R. Eirich, Ed., Vol. IV, Academic Press, New York, 1967, Chapter 5, pp 317–45.
(19) J. Fisher and A. G. Fredrickson, *Mol. Cryst. Liq. Cryst.*, **8**, 267 (1969).
(20) J. L. Ericksen, *Trans. Soc. Rheol.*, **13**, 9 (1969).

# Some Solution Properties of Polyacrylamide

**Petr Munk,* Tejraj M. Aminabhavi, Paul Williams, and Dolly E. Hoffman**

*Department of Chemistry, The University of Texas at Austin, Austin, Texas 78712*

**Miroslav Chmelir**

*Chemische Fabrik Stockhausen & Cie, Wissenschaftliches Labor, D-4150 Krefeld 1, Federal Republic of Germany.* *Received September 10, 1979*

ABSTRACT: Six samples of polyacrylamide prepared by radical polymerization in water solution were studied by the methods of sedimentation equilibrium and viscometry. Evaluation of sedimentation equilibrium yielded the molecular weight, the polydispersity parameter, and the second virial coefficient. The intrinsic viscosity increases with increasing concentration of sodium chloride. The parameters of the Mark–Houwink–Sakurada relation $[\eta] = KM^a$ were estimated and compared with the literature data.

Water-soluble polymers are rapidly gaining practical importance as viscosity-enhancing agents, flocculating agents, food additives, etc. However, at present the basic properties of these polymers and their solutions are not known to a satisfactory degree. This situation arises (among other things) from the fact that these polymers exhibit a large number of unwelcome properties. They frequently have broad distribution of molecular weights,

0024-9297/80/2213-0871$01.00/0 